

Identification of Contaminant Sources in Enclosed Spaces by a Single Sensor

Tengfei Zhang, Qingyan Chen^{*}

*Air Transportation Center of Excellence for Airliner Cabin Environmental Research (ACER),
School of Mechanical Engineering, Purdue University,
585 Purdue Mall, West Lafayette, IN 47907-2088, USA*

^{*} Corresponding author email: yanchen@purdue.edu

Abstract

To protect occupants from infectious diseases or possible chemical/biological agents released by a terrorist in an enclosed space, such as an airliner cabin, it is critical to identify gaseous contaminant source locations and strengths. This paper identified the source locations and strengths by solving inverse contaminant transport with the quasi-reversibility (QR) and pseudo-reversibility (PR) methods. The QR method replaces the second-order diffusion term in the contaminant transport equation with a fourth-order stabilization term. By using the airflow pattern calculated by Computational Fluid Dynamics (CFD) and the time when the peak contaminant concentration was measured by a sensor in downstream, the QR method solves the backward probability density function (PDF) of contaminant source location. The PR method reverses the airflow calculated by CFD and solves the PDF in the same manner as the QR method. The position with the highest PDF is the location of the contaminant source. The source strength can be further determined by scaling the nominal contaminant concentration computed by CFD with the concentration measured by the sensor. By using a two-dimensional and a three-dimensional aircraft cabin as examples of enclosed spaces, the two methods can identify contaminant source locations and strengths in the cabins if the sensors are placed in the downstream location of the sources. The QR method performed slightly better than the PR method but with a longer computing time.

Keywords: Inverse modeling; Computational fluid dynamics (CFD); Quasi-reversibility equation; Pseudo-reversibility equation; Backward location probability; Indoor environment.

Practical Implications

The paper presents a method that can be used to find a gaseous contaminant source location and determine its strength in enclosed spaces with the data of contaminant concentration measured by one sensor. The method can be a very useful tool to find where, what, and how the contamination has happened. The method is also useful for optimally placing sensors in enclosed spaces. The results can be applied to develop appropriate measures to protect

occupants in enclosed environments from infectious diseases or chemical/biological warfare agents released by a terrorist.

Nomenclature

$f(\vec{x};t)$	Forward probability density function of location	Δt	Positive time step
$f'(\vec{x};t)$	Backward probability density function of location	ΔV	Control volume
J	Mass flow rate	$\Delta \tau$	Negative time step
J'	Mass flow rate that is in opposite direction with J	Γ	Diffusion coefficient of gaseous contaminant scalar
S_ϕ	Source term	ε	Stabilization constant
t	Time, in ascending order	ϕ	Gaseous contaminant scalar
u_i	Velocity component in direction i	ρ	Air density
u_i'	Velocity component in direction i that is opposite to u_i	τ	Time, in descending order
\vec{x}	Position vector	Ω	Domain
x_i	Coordinate in direction i	<i>Subscripts</i>	
<i>Greek symbols</i>		i	Coordinate direction index
δ	Dirac delta function	f	Face index in an unstructured grid

Introduction

Without appropriate contaminant sensors in enclosed spaces, such as airliner cabins, airborne contaminant transport information cannot be obtained in a timely fashion to take protective actions. For example, Severe Acute Respiratory Syndrome (SARS) seems to be airborne (Li et al. 2007). If there were a sensor that could instantly detect SARS virus possibly released from the infected passenger in the flight from Hong Kong to Beijing in 2003 (Olsen et al., 2003), emergent measures could have been taken to protect other passengers from infection. The five fatalities of that flight might have been avoided as a result. If commercial liners are equipped with chemical/biological sensors that can tell what, when, where and how much contaminant is being released by a terrorist in an airliner cabin, airplanes would not be attractive targets for terrorist attacks (NRC, 2006). A sensor may detect in real time or with limited time delay the release of accidental contaminants in cabin air. The sensor provides crucial information to protect passengers and crew. However, most sensors for detecting infectious disease viruses and chemical/biological agents are expensive, bulky and heavy, so they cannot be deployed in a large quantity in airliner cabins. How to use the limited information from a few sensors to identify what, when, where and how much accidental contaminant has been released in a cabin is very challenging.

Airborne contaminant transport in an enclosed space, such as an airliner cabin, depends on airflow pattern. The airflow pattern is relatively stable even if there are occasional movements of passengers and crew (Mazumdar and Chen, 2007). With a known contaminant source location and strength, Computational Fluid Dynamics (CFD) can be used to study contaminant distribution in such an enclosed space. Horstman (1988) was possibly one of the first to use CFD to study steady-state contaminant transport in a two-dimensional aircraft cabin. Mizuno and Warfield (1992) also carried out similar studies on the distribution of contaminant (CO_2) in a three-dimensional aircraft mockup. Recently, Zhang and Chen (2007a) compared CO_2 transport in an airliner cabin with different ventilation strategies by CFD. Lin et al. (2005) simulated the unsteady airborne pathogen transport in a two-row section of a Boeing 767-300 aircraft cabin. The above studies show CFD can predict contaminant transport from its source to a location, such as sensor location. If we could reverse the CFD simulations, the contaminant source would be identified by the information from the sensor.

However, the inverse CFD modeling is ill-posed (Tikhonov and Arsenin, 1977) since it does not satisfy the solution stability (Alifanov, 1994). Thus to make inverse problems solvable, it is necessary to improve the solution stability. Both regularization (Tikhonov and Arsenin, 1977) and stabilization (Lattes and Lions, 1969) techniques can be used to stabilize the inverse governing transport equation. The regularization technique improves the solution stability by imposing a bound on the solution. The solution is obtained by minimizing the objective function with a regularized term. The stabilization technique introduces some stabilization terms into the reversed governing equations or solves some auxiliary equations to improve the solution stability. By comparing both the methods, Skaggs and Kabala (1995) concluded that the stabilization method used significantly less computational effort than the regularization method, although the stabilization method might provide slightly inferior results. So far the regularization method can only be applied in uniform flows (Atmadja and Bagtzoglou, 2001). Therefore, the stabilization method seems more appropriate.

Our previous study had used successfully the stabilization method for inverse CFD modeling to identify a contaminant source in an aircraft cabin (Zhang and Chen, 2007b). The quasi-reversibility (QR) method used in the study achieved stable solutions by replacing the second-order diffusion term in the CFD equations with a fourth-order term and by solving the new equations inversely. The QR method was first presented to solve ill-posed partial differential equations for heat conduction problems (Lattes and Lions, 1969; Clark and Oppenheimer, 1994). This method was also applied to reversely solve contaminant transport in groundwater to identify contaminant sources (Skaggs and Kabala, 1995; Bagtzoglou and Atmadja, 2003). Those results showed the contaminant source locations could be correctly identified, whereas the contaminant source strengths determined were dispersive. The QR method is still computationally demanding and is only conditionally stable depending on the coefficient used in the stabilization term.

Instead of reversing time, one can also solve inverse contaminant transport with reversed flows. This approach is called the pseudo-reversibility (PR) method. Kato et al. (2001; 2002; 2004) used the method to assess local pollution from upwind regions with backward trajectory analysis of the flows in atmospheric environment. The method has also been used in groundwater contaminant transport (Bagtzoglou et al. 1992; Wilson and Liu, 1994), where

both convection and diffusion transport of contaminant is solved with reversed flows. The PR method is easy to implement and the results are reasonable in many applications. However, when the diffusion is dominant in contaminant transport, its accuracy is poor.

Most importantly, both the QR and PR methods require accurate airflow and contaminant distributions in the flow domain as the initial conditions. For many enclosed spaces, including aircraft cabins, the airflow distribution does not change much and can be obtained by CFD simulation with appropriate thermo-fluid boundary conditions that are often known in advance. However, the initial contaminant concentration field is unknown. Since most of sensors are expensive, bulky and heavy, the applications of QR or PR method relying on lots of sensors to measure initial contaminant concentration distributions are not practical.

On the other hand, there are successful studies in identifying contaminant sources with limited quantity of sensors together with the optimization and probability methods. The optimization method (Khemka et al. 2006; Laird et al. 2006) used forward modeling to obtain the distributions of contaminant concentrations based on all possible contaminant sources. Then they optimized a solution best-fitted with the corresponding measured data at all sensor locations. Because plausible combinations of possible source locations and strengths are huge, this approach involves a large amount of forward modeling. The probability approach uses probability to express a potential contaminant source. In groundwater transport, Neupauer and Wilson (1999; 2001; 2004; 2005) used backward location probability which illustrates the likely position of a solute particle in the previous time to show the contaminant source location. The governing equations solved were the very complicated adjoint-state equations. However, the backward location probability can still be valuable.

With similarities between solute particle transport in groundwater and contaminant transport in an enclosed space, it seems possible to use the QR and PR methods together with the backward location probability to achieve the objective of our study. The objective is to use the information obtained from one sensor to determine when, where, and how much the contaminant is released in an enclosed space. This paper details the research effort and the results.

Research Approach

This section presents the fundamentals of identifying the contaminant source location and strength by using the QR and PR methods with the information measured by a single sensor.

Identification of contaminant source location based on a single sensor

As reviewed in the previous section, backward location probability can be useful to identify contaminant source location. Before discussing the details on backward location probability, let us introduce forward location probability first.

Forward location probability represents the chances of contaminant appearing at a specified location after it has been released from a source (Dagan, 1987; Jury and Roth, 1990). Take an example of particle transport in a two-dimensional flow as shown in Figure 1(a). A

downstream sensor detects the particle plume with some time delay ($t=t_0$) after the source released instantaneously at $t=0$. The particle concentration at the sensor location reflects the possibility of particles appearing at the sensor location. For simplicity, this paper considered particle as “gas” so that the transport of particles is the same as gases. The higher the concentration at a location, the more possible the particles appear at the location. Mathematically, the forward location probability density function (PDF) at time, t , can be expressed as (Neupauer and Wilson, 2001),

$$f(\vec{x};t) = \frac{\phi(\vec{x};t)}{\int_{\Omega} \phi(\vec{x};0^+) d\Omega} \quad (1)$$

where $f(\vec{x};t)$ is the forward location PDF at position \vec{x} and time t , $\phi(\vec{x};t)$ is the local contaminant concentration, $\int_{\Omega} \phi(\vec{x};0^+) d\Omega$ is the total contaminant released. If none of the contaminant has been extracted out of the domain since the release, the integration of Equation (1) in the space should be equal to one. Although Equation 1 was derived from particle contaminant transport, it can also be used for gaseous contaminants.

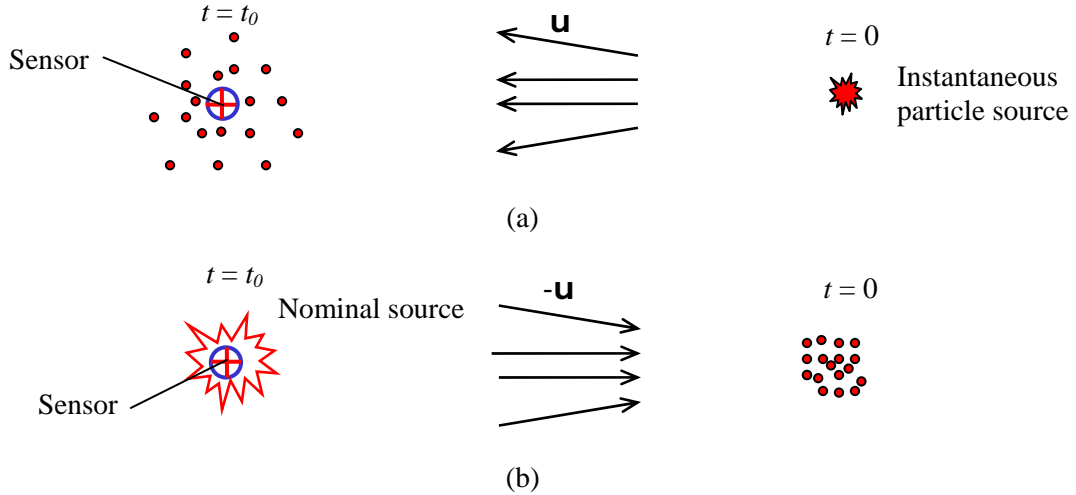


Fig. 1 Particle transport in a two-dimensional flow to illustrate location probability (a) forward transport, (b) backward transport

To calculate forward location PDF, the governing equation of contaminant transport should be solved to obtain local concentration. Although contaminants in enclosed spaces can exist in gaseous, liquid droplet, and solid particle forms, this paper deals with only gaseous contaminant for simplicity. The governing transport equation for a gaseous contaminant is,

$$\frac{\partial[\phi(t)]}{\partial t} = -\frac{\partial}{\partial x_i} [u_i \phi(t)] + \frac{\partial}{\partial x_i} \left[\frac{\Gamma}{\rho} \frac{\partial \phi(t)}{\partial x_i} \right] + S_{\phi} \quad (2)$$

The left hand side of the above equation is the contaminant concentration change rate, and the right hand side of the equation is the convection, diffusion and source terms, respectively. By combining Equation 1 and 2, the forward location PDF can be solved.

Similarly, the backward location probability can be explained by using the example of particle transport in the two-dimensional flow as shown in Figure 1(a). Once the sensor has detected the particle plume at time, t_0 , one can release a nominal source at the sensor location and solve reversely contaminant transport as shown in Figure 1(b). The chances of contaminant appearing at a location in the previous time ($t < t_0$) can be expressed by the backward location probability. The backward PDF can be calculated as,

$$f'(\vec{x};t) = \frac{\phi(\vec{x};t)}{\int_{\Omega} \phi(\vec{x};t_0^-) d\Omega} \quad (3)$$

where $f'(\vec{x};t)$ is the backward location PDF, $\phi(\vec{x};t)$ is the backward contaminant concentration due to the nominal source, $\int_{\Omega} \phi(\vec{x};t_0^-) d\Omega$ is the total contaminant released at $t=t_0$ at the sensor location. Since the higher the PDF, the more possible the contaminant appears at a location, the position with the highest backward PDF at $t=0$ should be the contaminant source location. Thus the contaminant source location can be identified with the backward location PDF.

To calculate backward location PDF with Equation 3, the distribution of backward contaminant concentration due to release of the nominal source is required. However Equation 2 cannot be used to solve for the distribution since it is inversely unstable. By discretizing Equation 2 with a negative time step, $\Delta\tau$, one will find that the calculation error of $\phi(\tau)$ would be accumulated and amplified with the elapse of time in reverse direction and the solution loses stability (Zhang and Chen, 2007b). The reason is that in forward modeling the contaminant transport is spontaneously transported from high concentration at the current time to low concentration at the following time. However, in inverse modeling to solve for the contaminant transport in the previous time the contaminant needs to be transported from low concentration at the current time to high concentration at the previous time that is impossible. To make inverse contaminant transport solvable, this study proposes to solve the quasi-reversibility (QR) and pseudo-reversibility (PR) equations together with Equation 3.

The quasi-reversibility equation

One method to obtain a stable solution of the backward contaminant concentration due to the nominal source is by replacing the second-order diffusion term in Equation 2 with a fourth-order term. In the meanwhile, the nominal source at the sensor location is also required to be reflected in the QR equation thus yielding,

$$\frac{\partial[\phi(\tau)]}{\partial\tau} = -\frac{\partial}{\partial x_i} [u_i \phi(\tau)] + \varepsilon \frac{\partial^2}{\partial x_i^2} \left[\frac{\partial^2 \phi(\tau)}{\partial x_i^2} \right] + S_{\phi} \delta(\vec{x} - \vec{x}_0) \delta(\tau - \tau_0) \quad (4)$$

where ε is the stabilization coefficient, \vec{x}_0 is the sensor location, $\tau_0 (=t_0)$ is the time when the peak contaminant concentration is detected at the fixed sensor location. The last term on the right-hand side of Equation 4 is the nominal instantaneous source at the sensor location.

With an appropriate ε , the error of $\phi(\tau)$ in the discretized format of Equation 4 can be damped with the elapse of time in reverse direction, so the solution scheme becomes stable. In other words, the stabilization term acts like an “engine” to compel the reverse transport of contaminant and thus obtains stability. With the continuous contribution from the stabilization term, the contaminant mass in the domain is not conservative anymore, i.e. Equation 4 is not conservative. In addition, Equation 4 is conditionally stable depending on the value of ε . The QR method is still computationally demanding with the discretizing of the fourth-order stabilization term.

The pseudo-reversibility equation

Instead of reversing time as the QR method, the PR method solves the inverse contaminant transport by reversing flows with the following equation,

$$\frac{\partial[\phi(t)]}{\partial t} = -\frac{\partial}{\partial x_i} [u_i' \phi(t)] + S_\phi \delta(\vec{x} - \vec{x}_0) \delta(t - t_0) \quad (5)$$

where t is the time in ascending order ($\Delta t > 0$) but u_i' is a reversed velocity component whose direction is opposite to u_i . The diffusion term in Equation (5) is neglected to decrease the dispersive effect, since the ideally reverse contaminant transport should be without diffusion. Because the time step, Δt , is positive in Equation (5), the discretized equation is stable with the time-implicit scheme as normally used in Equation 2 for forward modeling.

To calculate the backward PDF with Equation 4 or 5 together with Equation 3, the information required from a sensor is its location (\vec{x}_0) and the contaminant transport time (t_0) from the moment the source started to release to the moment that the peak contaminant concentration was detected by the sensor. The measured concentration at the sensor is not needed in identifying the contaminant source location with backward PDF. However, the measured concentration is used to identify the contaminant source strength that will be discussed later in this paper.

Numerical methods

The numerical scheme based on unstructured meshes is usually used to simulate the contaminant transport by CFD in an enclosed space with complex geometry, such as an aircraft cabin. A numerical scheme for unstructured meshes should work for structured meshes since structured meshes are special cases of unstructured meshes. This paper illustrates a numerical scheme for unstructured meshes that are more generic by using a two-dimensional domain with two triangular unstructured cells as shown in Figure 2. Cells c_0 and

$c1$ share a common face f . The contaminant concentrations are calculated in the cell centers with ϕ_0 as the concentration for Cell $c0$, and ϕ_1 for Cell $c1$.

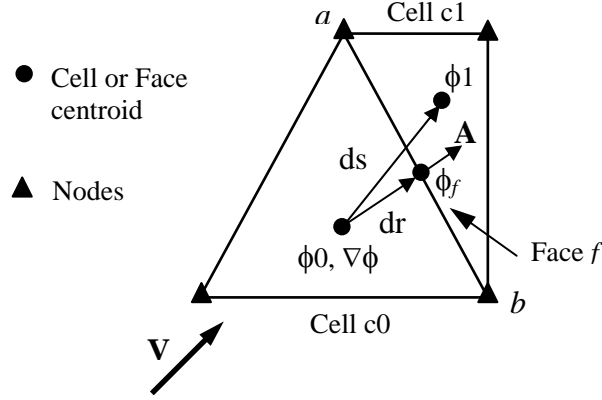


Fig. 2 Two adjacent cells $c0$ and $c1$ in a two-dimensional flow domain

By integrating Equation (4) over the cell volume and time step and by using backward-time implicit concentration to represent the right-hand side of Equation (4), the contaminant concentration at the previous time step can be obtained by the following discretized equation,

$$\begin{aligned} \phi(\tau + \Delta\tau) = \phi(\tau) + \frac{1}{\rho\Delta V} \left[\sum_f J_f \phi_f(\tau + \Delta\tau) \right] \Delta\tau + \\ \varepsilon \Delta\tau \frac{\partial^2}{\partial x_i^2} \left[\frac{\partial^2 \phi(\tau + \Delta\tau)}{\partial x_i^2} \right] + S_\phi \Delta\tau \cdot \delta(\vec{x} - \vec{x}_0) \delta(\tau - \tau_0) \end{aligned} \quad (6)$$

Note the time step, $\Delta\tau$, in the above equation is negative in inverse modeling. The second term of the right hand side of Equation (6) is the convection term where the face concentration, ϕ_f , can be calculated by the linear reconstruction method (Mathur and Murthy, 1997); and the third term is the stabilization term that can be calculated by using the formula suggested by Zhang and Chen (2007b). The face flow rate J_f is obtained from airflow distribution.

Similarly, Equation (5) can be discretized as,

$$\phi(t + \Delta t) = \phi(t) + \frac{1}{\rho\Delta V} \left[\sum_f J'_f \phi_f(t + \Delta t) \right] \Delta t + S_\phi \Delta t \cdot \delta(\vec{x} - \vec{x}_0) \delta(t - t_0) \quad (7)$$

where J'_f in Equation (7) is opposite to J_f in Equation (6).

The above numerical schemes are applicable to a three-dimensional space. This study has implemented the numerical schemes for both the QR and PR equations into a commercial CFD program, FLUENT (<http://www.fluent.com/>), as a user defined function.

Results and Discussion

To apply both the QR and PR methods for identifying contaminant sources in enclosed spaces, this study first used a two-dimensional empty aircraft cabin and then a three-dimensional cabin. The two-dimensional cabin case is simple and fast to obtain results and the three-dimensional case is more realistic.

Contaminant source identification in a two-dimensional aircraft cabin

The environmental control systems for modern commercial airliners create a very strong flow in a cross section and minimize flow along the longitudinal direction. The airflow in an aircraft cabin is close to two dimensional. Thus, our study has tested the QR and PR methods in a two-dimensional, empty aircraft cabin as shown in Figure 3. The simplified interior geometry would eliminate errors caused by furniture, occupants, heat sources, etc. The aircraft cabin was 4.72 m wide and 2.10 m high. Conditioned air was supplied from the two linear slot inlets at the ceiling, and the air was extracted from the outlets at the side walls near the floor level. There was no heat generated in this cabin model so the airflow in the cabin can be considered as isothermal. A contaminant was released in the cabin from $t=0.0$ s to $t=0.04$ s. Two release locations were considered: one on the left cabin floor and another in the left upper cabin as shown in Figure 3. The flow domain was created with unstructured meshes with *Pave* scheme using GAMBIT (<http://www.fluent.com/>). The grid size was around 0.05 m.

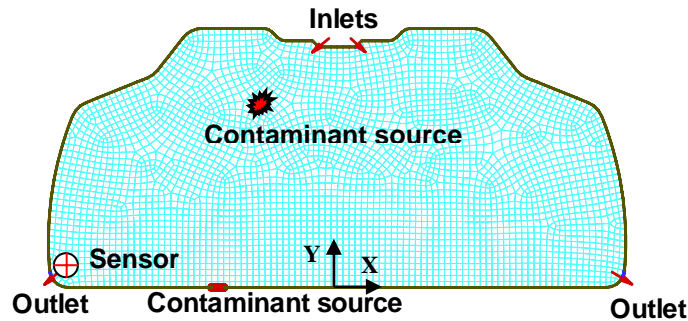


Fig. 3 Schematic of inverse modeling in a two-dimensional aircraft cabin

The inverse modeling needs the airflow distribution and unsteady contaminant concentration measured by a sensor. This paper used CFD to obtain the airflow distribution for the inverse modeling. The sensor information of contaminant concentration versus time was also simulated by using the unsteady CFD computation, although in reality it should be measured by a sensor.

The CFD computation solved a set of governing partial differential RANS (Reynolds-averaged Navier-Stokes) equations with appropriate boundary conditions. These governing equations include continuity, momentum, contaminant concentration, turbulent kinetic energy, and dissipation rate of turbulent kinetic energy. The renormalization group (RNG) k - ϵ model was used for the turbulent flow. These partial differential equations were discretized into algebraic equations by using the finite volume method with a second-order upwind scheme.

Because the equations were highly nonlinear, iterations were needed to achieve converged solutions. According to the guideline of using CFD for indoor environment modeling (Chen and Srebric, 2002), the CFD program and users should be validated. Due to limited space available for this paper, the readers can refer to our another paper (Zhang and Chen, 2007a) that show the validation.

Figure 4 shows the information needed for the inverse modeling. The CFD modeling calculated the airflow pattern in the cabin and the concentration versus time representing the measured concentration by a sensor near the left outlet. This sensor was deployed for the demonstration of the inverse modeling, which does not mean the sensor must be located at the outlet position in actual operation. According to Mazumdar and Chen (2007), the optimal sensor location should be in the middle of the ceiling in an aircraft with such an air distribution system. The airflow pattern on the left cabin is counter-clockwise as shown in Figure 4(a). It took about 10 s for the contaminant to reach the outlet, so the contaminant concentration reached its peak at the sensor location at about $t=10$ s as shown in Figure 4(b).

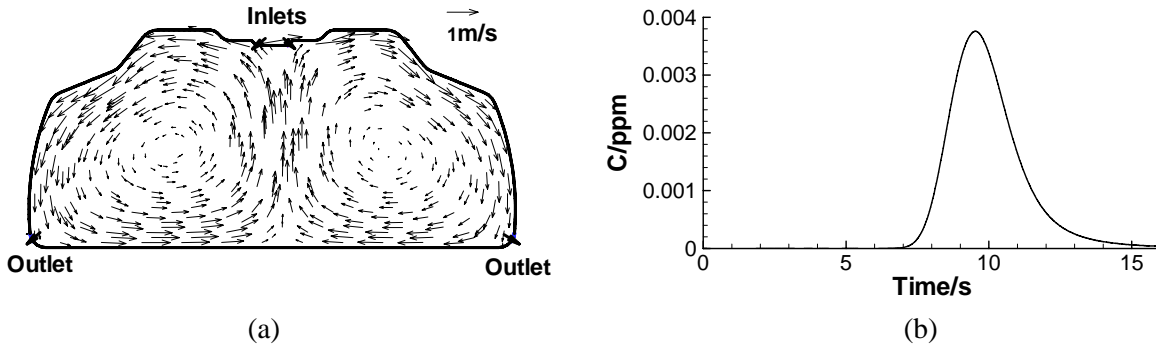


Fig. 4 Information needed for the inverse modeling (a) steady-state airflow pattern, (b) unsteady contaminant concentration at the sensor location that shows a peak

With the airflow distribution (Fig. 4a) as initial conditions, the inverse simulation started at $t=10$ s with a nominal source released instantaneously at the sensor location. The distribution of backward location PDF at $t=0$ was obtained by using both the QR and PR methods. The QR equation used a stabilization coefficient of 0.6×10^{-5} according to the guideline recommended in our earlier studies (Zhang and Chen, 2007b). The simulations were conducted in a personal computer with a Pentium 2.6 GHz processor and 1 Gb of memory. It took about 100 minutes to complete the QR simulation and around 30 minutes for the PR simulation. The QR method used much longer time because of the fourth-order stabilization term. Figure 5 shows the contaminant source location identified by the two methods, with the highest PDF value illustrating the source location. The PDF values in Figure 5 have been normalized to make the integral location probability in the flow domain be equal to one. This is because during the inversion a part of nominal contaminant was exhausted to the outside through the inlets. Additionally the QR equation may not conserve when the second-order diffusion term is replaced by the fourth-order stabilization term. Therefore, the normalization is necessary.

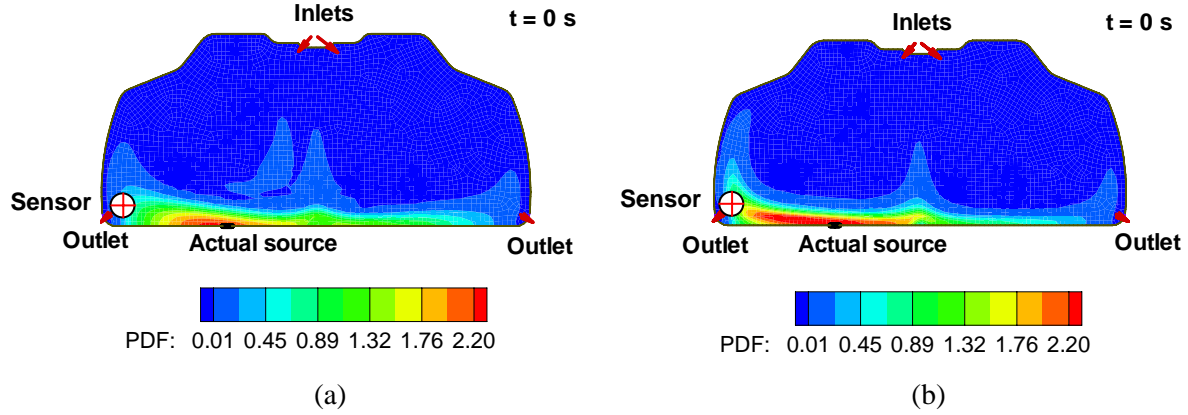


Fig. 5 Contaminant source location identified by the highest PDF and its comparison with the actual source location illustrated by the black bar (a) by the QR method and (b) by the PR method

Both the results obtained by the QR and PR methods look dispersive. The distribution of backward PDF could not be ideally concentrated to a small region around the actual source location as shown in Figure 5. The reason is that the fourth-order term in the QR equation can not completely reverse the diffusion effect. The PR method reversed the flow but not the diffusion. Thus, the dispersion is unavoidable. Nevertheless, the contaminant source location identified by the two methods was quite close to the actual one. A closer look at the results concludes that the QR method is slightly better than the PR method as compared in Table 1.

Table 1 Comparison of contaminant source location identified by the QR and PR methods

	X	Y
Actual location (Location 1)	-1.05 m	0.024 m
Location identified by the QR method (Location 2)	-1.24 m	0.024 m
Location identified by the PR method (Location 3)	-1.60 m	0.075 m

With the source location identified, a CFD simulation can be run to obtain the contaminant concentration versus time with another nominal source released at the identified location. Since the contaminant concentration depends linearly on the contaminant strength, the linear scale-up or scale-down of the nominal source strength can be used to determine the actual source strength. By comparing the contaminant concentration simulated by CFD with the measured concentration at the sensor location, such as the one shown in Fig. 4b, the contaminant strength can be identified by

$$S_{\phi} = \frac{\phi_m}{\phi_n} S_{\phi,n} \quad (8)$$

where ϕ_m is the measured contaminant concentration, ϕ_n is the simulated concentration from the nominal source, $S_{\phi,n}$ is the nominal contaminant source strength. ϕ_m and ϕ_n can also be the averaged concentration in a time slot. To illustrate the application, Figure 6 shows the

contaminant concentration versus time when contaminant sources were released with the same strength at the three locations as shown in Table 1. The differences among them are negligible. Therefore, the source location and strength can be determined with the QR or PR method. Although not explicitly stated, the time of release is also identified. For this particular case, it was about 10 s earlier than when the sensor measured the peak contaminant concentration.

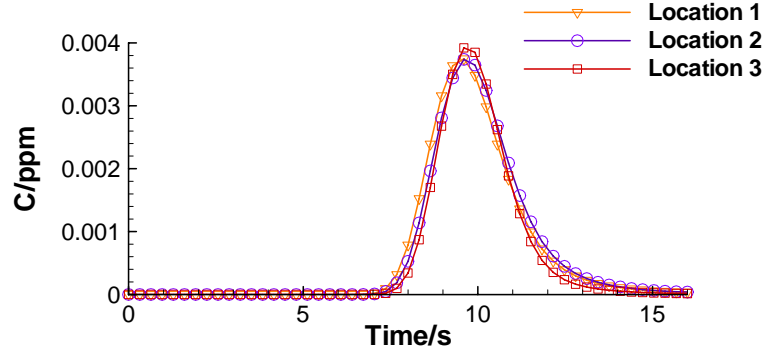


Fig. 6 Contaminant concentration versus time at the sensor when a contaminant source was released at the three locations.

The above results show that both the QR and PR methods can identify the contaminant source released on the left cabin floor. With the sensor placed at the left outlet, would the two methods be able to identify a contaminant source released somewhere else rather than on the cabin floor? To answer this question, another case was studied for a source released inside the left cabin as shown in Figure 3. Similar to the previous case, the measured contaminant concentration at the sensor location should be known in advance. Figure 6(a) shows the unsteady concentration simulated by forward CFD modeling to represent the measured one. Within 20 seconds the contaminant was circulated nearly two cycles in the cabin, the contaminant concentration “measured” at the left outlet shows only one peak at $t=15$ s. This is because in the first cycle the concentration at the sensor location was too low to be measured. Figure 7(b) shows the simulated contaminant concentration distribution at $t=15$ s. Clearly the sensor was not able to measure the maximum concentration in the cabin because it was not placed in the right downstream location of the contaminant source.

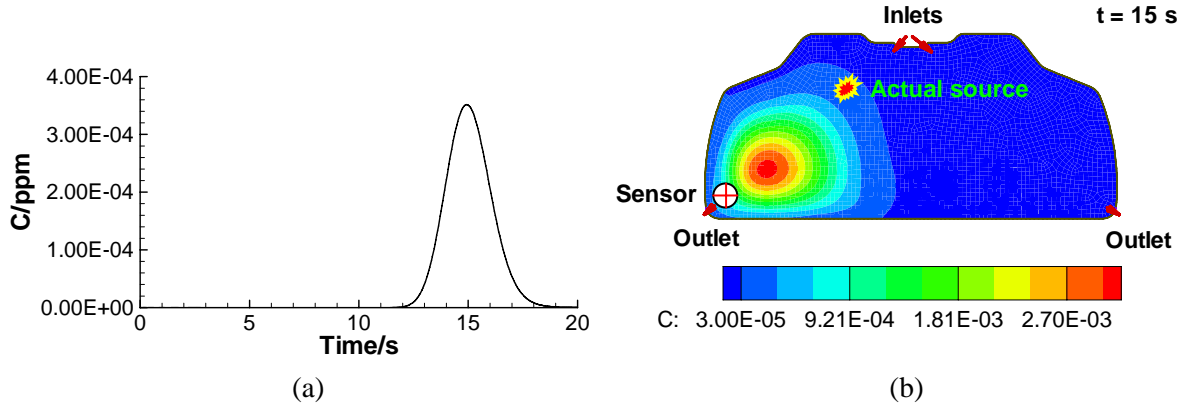


Fig. 7 Contaminant concentration for the source released inside the cabin (a) “measured” at the sensor location, (b) distribution in the cabin at $t=15$ s

With the airflow pattern as shown in Figure 4(a) and the unsteady contaminant concentration at the sensor location as shown in Figure 7(a), a nominal source was released instantaneously at the sensor location and the distribution of backward PDF was reversely simulated to from $t=15$ s to $t=0$ s. The computation time for the QR simulation was about 150 minutes, and for the PR method around 45 minutes. Figure 8 shows the distribution of backward PDF at $t=0$ s obtained by the two methods. The contaminant source location identified by the QR method is in a small region close to the left ceiling, while the PR method identified a much large area in the same location. Clearly, the sensor location in this case is inappropriate so that neither method was able to identify the contaminant source location. However, if the sensor is located in the center of the contaminant plume (Sensor 2 in Figures 8(c) and 8(d)), the two methods can identify correctly the contaminant source location as shown in the figures. The results from the PR method are a little more dispersive than those from the QR method.

The above results indicate that identification of contaminant source location and strength based on a single sensor with the QR or PR methods is possible if the sensor is appropriately placed in the downstream location of the contaminant source. Otherwise, multiple sensors are needed.

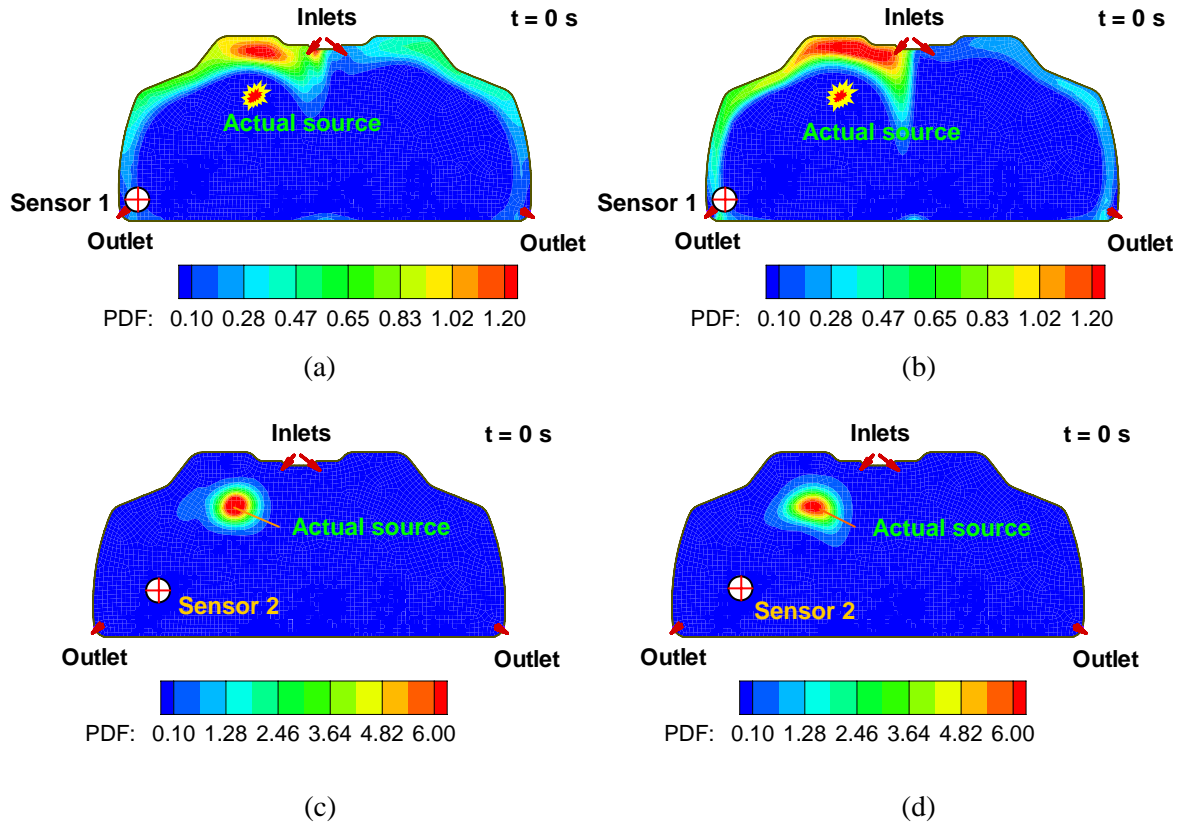


Fig. 8 Contaminant source location identified (a) by sensor 1 with the QR method, (b) by sensor 1 with the PR method, (c) by sensor 2 with the QR method, and (d) by sensor 2 with the PR method

Contaminant source identification in a three-dimensional aircraft cabin

This study has tested further the QR and PR methods for a three-dimensional mockup of a twin-aisle aircraft cabin as shown in Figure 9. The mockup had four-row seats with 50% of occupancy rate. Fourteen heated manikins with box shape were used to simulate the seated passengers. Air was supplied at the ceiling level from linear slot diffusers and exhausted from the outlets at the floor level on the side walls. This investigation has studied two cases. Case 1 was to identify a contaminant source (source 1) from the head level of the middle passenger in the third row by a sensor (sensor 1) located above the passenger near the ceiling. Case 2 was for a contaminant source (source 2) from the leg level of a passenger seated next to the window in the first row with a sensor (sensor 2) located in the central ceiling of the first row. Both contaminant sources were released from $t=0.0$ to 0.04 s.

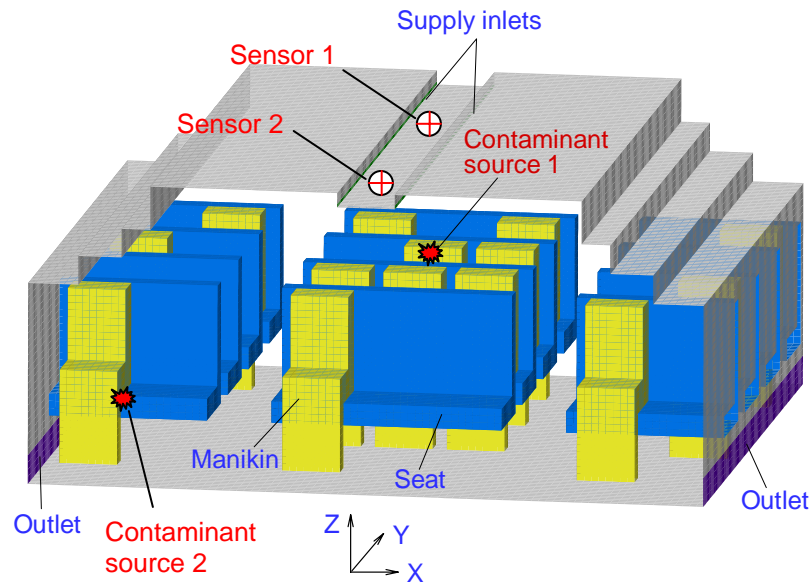


Fig. 9 Schematic of inverse modeling for a three-dimensional aircraft cabin

The two cases used structured quad-cells for the aircraft cabin. With the structured cells, the curved cabin geometry was represented by the stair-shape one. This is to reduce the discretization errors of the fourth-order term in the QR equation. The cell size was about 0.05 m. The same as those for the two-dimensional aircraft cabin, CFD modeling was used to obtain the airflow data and the transient contaminant concentrations measured by the sensors as shown in Figure 10. Although the contaminant source strengths were the same, the contaminant concentration measured by sensor 1 was much higher than that by sensor 2 because sensor 1 was placed right above contaminant source 1.

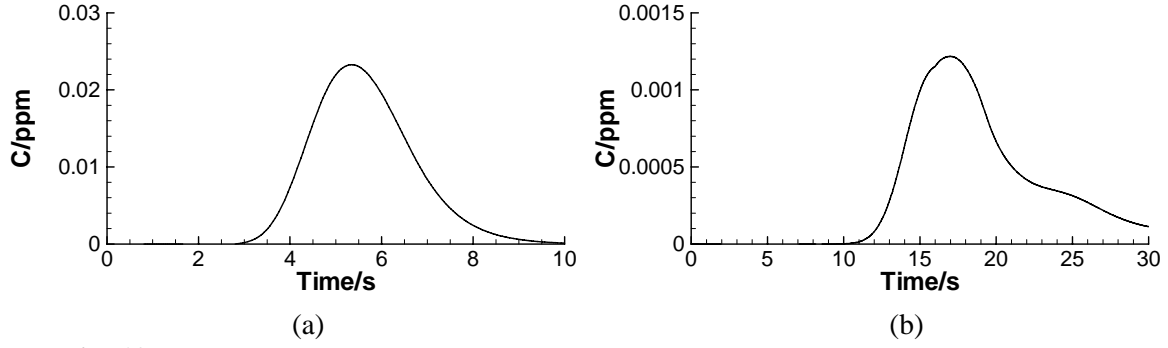


Fig. 10 Contaminant concentration at the sensor locations (a) for contaminant source 1 by sensor 1 and (b) for contaminant source 2 by sensor 2

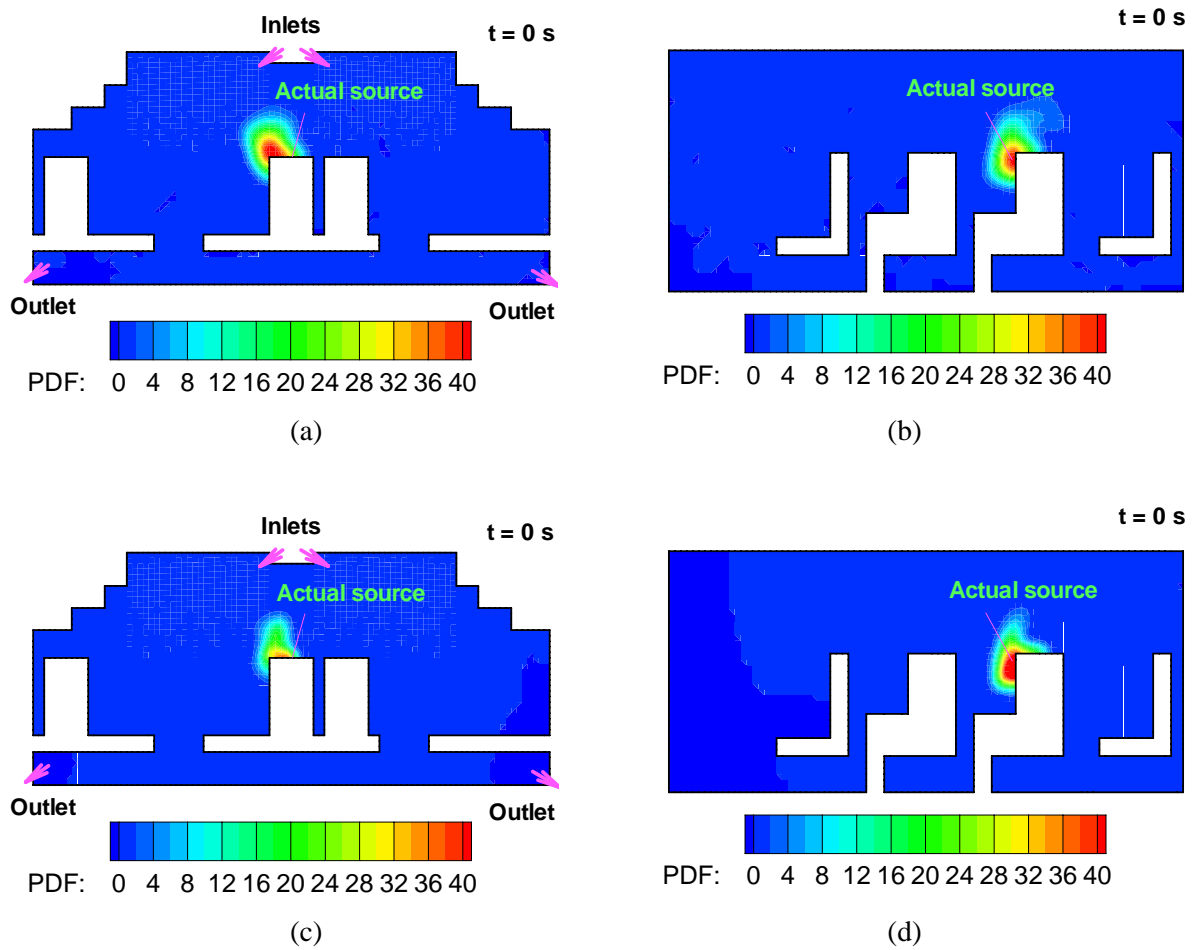


Fig. 11 Location of contaminant source 1 identified (a) in the cross section through the third row by the QR method, (b) in the mid-longitudinal section by the QR method, (c) in the cross section through the third row by the PR method, and (d) in the mid-longitudinal section by the PR method

The inverse simulation for Case 1 was performed by adding an instantaneous nominal source at the sensor location at $t=5.5$ s when the sensor measured the peak contaminant concentration. The QR method used 0.475×10^{-5} as the stabilization coefficient. The

computation was conducted on a Linux computer with an AMD 64 processor (1.8 GHz) and 2 GB of memory. It took about 60 hours for the QR method and 17 hours for the PR method to complete the simulations. One reason for such long computation time was that the numerical solution used Gauss-Seidel iteration without implementing multigrid acceleration at the current stage. Figure 11 shows the corresponding distributions of backward PDF at $t=0$ s in two different planes for the two methods. Both methods were able to identify the source location. The results by the QR method are slightly better than those by the PR method, although the difference is minimal.

For Case 2, it took a long time for the contaminant to be transported from the source to the sensor. As shown in Figure 10(b), the sensor detected the peak concentration at $t=17$ s. With the same approach as that for Case 1, the results for Case 2 are shown in Figure 12. The distribution of backward PDF at $t=0$ s is quite dispersive by the inverse simulations. Although the results are not as good as those for Case 1, the two methods can still identify the contaminant source.

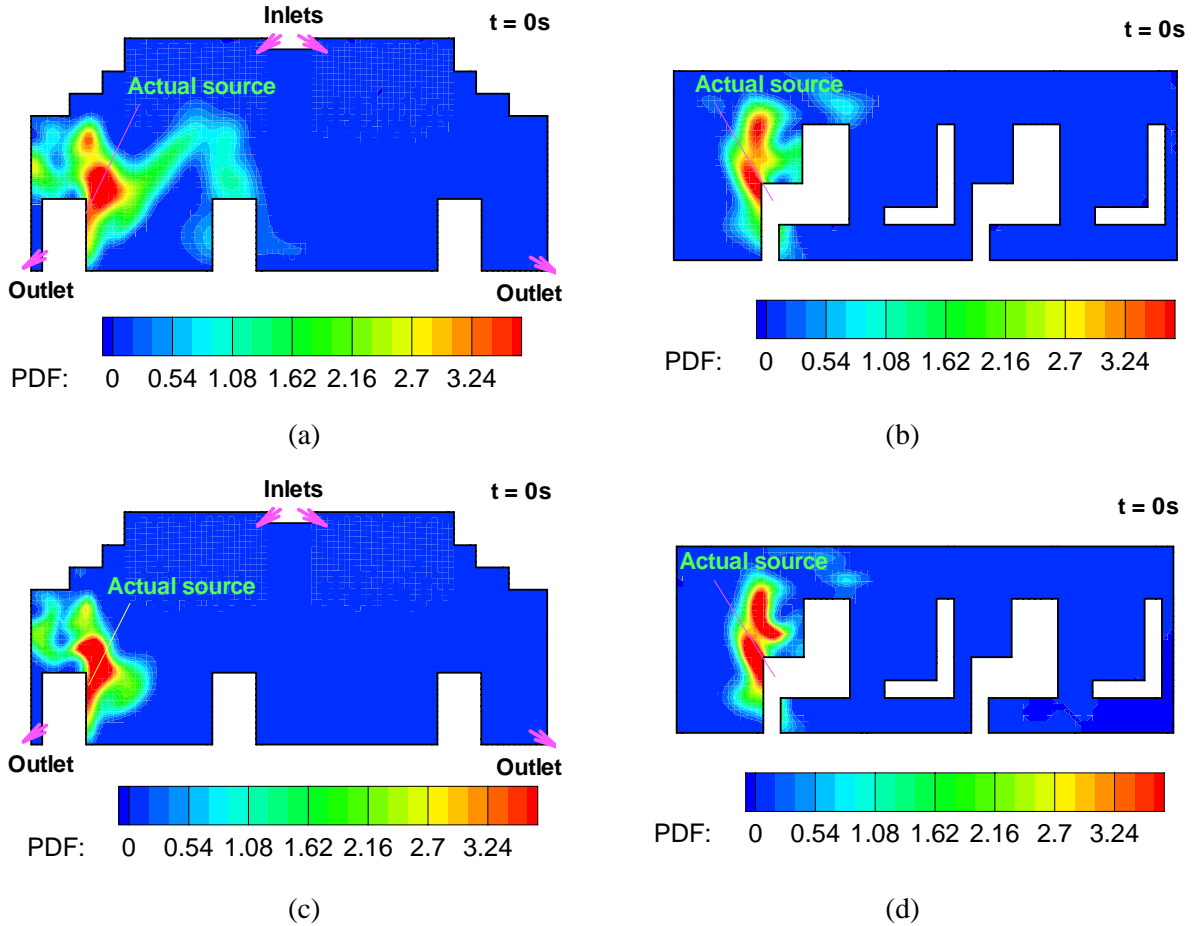


Fig. 12 Location of contaminant source 2 identified (a) in the cross section through the first row by the QR method, (b) in the longitudinal section by the QR method, (c) in the cross section through the first row by the PR method, and (d) in the longitudinal section by the PR method

Similar to the cases of the two-dimensional aircraft cabin, the strengths of both contaminant sources can also be identified with linear scaling comparison by running forward

simulations with nominal sources released at the identified locations. The results are not shown due to limited space available in this paper.

Finally but not least, the QR and PR method developed in this paper is for common contaminant detection in enclosed spaces. The methods can be used for indoor spaces. However, the air change rate in an aircraft cabin is 20 to 30 ACH that is convection dominant while that in a typical indoor environment is around 5 ACH where diffusion cannot be neglected. The theory shown in the paper indicates that the accuracy of the methods for indoor space would be poorer than that for aircraft cabin.

Conclusions

This study used the quasi-reversibility (QR) and pseudo-reversibility (PR) methods to identify gaseous contaminant source locations and strengths in enclosed spaces, such as airliner cabins. The methods solved backward probability density function (PDF) of contaminant sources, which can be linked to the source locations. The source strengths were determined by using a CFD simulation and the scaling of the computed contaminant concentration with the measured one. By applying the two methods to a two-dimensional and a three-dimensional aircraft cabin, the following conclusions could be drawn:

- (1) Both the QR and PR methods can identify the location of a contaminant source with a stable airflow pattern and measured contaminant concentration over time by a single sensor. It is very important that the sensor must be placed in the downstream location of the contaminant source.
- (2) The distribution of backward PDF is dispersive for the two methods because of the approximations used for the diffusion term of the governing contaminant transport equation. The longer the simulation time, the more dispersive the results.
- (3) The QR method is slightly better than the PR method. However, the QR method needs longer computing time because the solution of the fourth-order stabilization term is computationally demanding.

Acknowledgements

This project is funded by the U.S. Federal Aviation Administration (FAA) Office of Aerospace Medicine through the Air Transportation Center of Excellence for Airliner Cabin Environment Research under Cooperative Agreement 04-C-ACE-PU. Although the FAA has sponsored this project, it neither endorses nor rejects the findings of this research. The presentation of this information is in the interest of invoking technical community comment on the results and conclusions of the research.

References

- Alifanov, O.M. (1994) *Inverse heat transfer problems*, New York, Springer-Verlag.
- Atmadja, J. and Bagtzoglou, A.C. (2001) State of the art report on mathematical methods for groundwater pollution source identification, *Environ. Forens.*, **2**, 205-214.

- Bagtzoglou, A.C., Dougherty, D.E. and Tompson, A.F.B. (1992) Application of particle methods to reliable identification of groundwater pollution sources, *Water Resour. Manage.*, **6**, 15-23.
- Bagtzoglou, A.C. and Atmadja, J. (2003) Marching-jury backward beam equation and quasi-reversibility methods for hydrologic inversion: Application to contaminant plume spatial distribution recovery, *Water Resour. Res.*, **39**, SBH101-SBH1014.
- Chen, Q. and Srebric, J. (2002) A procedure for verification, validation and reporting of indoor environment CFD analyses, *HVAC&R Research.*, **8**, 201-216.
- Clark, G.W. and Oppenheimer, S.F. (1994) Quasireversibility methods for non-well-posed problems, *Elec. J. Diff. Equations*, **8**, 1-9.
- Dagan, G. (1987) Theory of solute transport by groundwater, *Annu. Rev. Fluid Mech.*, **19**, 183-215.
- Fluent. (2005) *Fluent 6.2 UDF manual*, Fluent Inc.
- Horstman, R.H. (1988) Predicting velocity and contaminant distribution in ventilated volumes using Navier-Stokes equations. *Proceedings of the ASHRAE Conference IAQ 88, April 11-13*. Atlanta, Georgia, 209-230.
- Jury, W.A. and Roth, K. (1990) *Transfer function and solute movement through soil: Theory and applications*, Basel, Switzerland, Birkhäuser Verlag.
- Kato S., Pochanart P. and Kajii Y. (2001) Measurements of ozone and nonmethane hydrocarbons at Chichi-jima island, a remote island in the western Pacific: long-range transport of polluted air from the Pacific rim region, *Atmos. Environ.*, **35**, 6021-6029.
- Kato S., Pochanart P., Hirokawa J., Kajii Y., Akimoto H., Ozaki Y., Obi K., Katsuno T., Streets D.G. and Minko N.P. (2002) The influence of Siberian forest fires on carbon monoxide concentrations at Haplo, Japan, *Atmos. Environ.*, **36**, 385-390.
- Kato S., Kajii Y., Itokazu R., Hirokawa J., Koda S. and Kinjo Y. (2004) Transport of atmospheric carbon monoxide, ozone, and hydrocarbons from Chinese coast to Okinawa island in the Western Pacific during winter, *Atmos. Environ.*, **38**, 2975-2981.
- Khemka A., Bouman C.A. and Bell, M.R. (2006) Inverse problems in atmospheric dispersion with randomly scattered sensors, *Digit. Signal Process.*, **16**, 638-651.
- Laird, C.D., Biegler, L.T. and van Bloemen Waanders, B.G. (2006) Mixed-integer approach for obtaining unique solutions in source inversion of water networks, *J. Water Resour. Plan. Manage.*, **132**, 242-251.
- Lattes, R. and Lions, J.L. (1969) *The method of quasi-reversibility, applications to partial differential equations*, New York, Elsevier.
- Li, Y., Leung, G.M., Tang, J.W., Yang, X., Chao, C.Y.H., Lin, J.Z., Lu, J.W., Nielsen, P.V., Niu, J., Qian, H., Sleigh, A.C., Su, H.-J. J., Sundell, J., Wong, T.W., and Yuen, P.L. 2007. Role of ventilation in airborne transmission of infectious agents in the built environment – a multidisciplinary systematic review, *Indoor Air*, **17**, 2–18
- Lin, C.H., Horstman, R.H., Ahlers, M.F., Sedgwick, L.M., Dunn, K.H., Topmiller, J.L., Bennett, J.S. and Wirogo, S. (2005) Numerical simulation of airflow and airborne pathogen transport in aircraft cabins - Part 2: Numerical simulation airborne pathogen transport, *ASHRAE Trans.*, **111**, 764-768.
- Mathur, S.R. and Murthy, J.Y. (1997) A pressure-based method for unstructured meshes, *Numer. Heat Tr. B*, **31**, 195-215.
- Mazumda, S. and Chen, Q. (2007) Influence of thermal loading patterns on placement of contaminant detection sensors in a commercial aircraft cabin, *Environ. Eng. Sci.*, Submitted.
- Mizuno, T. and Warfield, M.J. (1992) Development of three-dimensional thermal airflow analysis computer program and verification test, *ASHRAE Trans.*, **98**, 329-338.

- Neupauer, R.M. and Wilson J.L. (1999) Adjoint method for obtaining backward-in-time location and travel time probabilities of a conservative groundwater contaminant. *Water Resour. Res.*, **35**, 3389-3398.
- Neupauer, R.M. and Wilson J.L. (2001) Adjoint-derived location and travel time probabilities for a multidimensional groundwater system. *Water Resour. Res.*, **37**, 1657-1668.
- Neupauer, R.M. and Wilson J.L. (2004) Forward and backward location probabilities for sorbing solutes in groundwater. *Adv. Water Resour.*, **27**, 689-705.
- Neupauer, R.M. and Wilson J.L. (2005) Backward probability model using multiple observations of contamination to identify groundwater contamination sources at the Massachusetts Military Reservation. *Water Resour. Res.*, **41**, W02015, 1-14.
- NRC (National Research Council). (2006) *Defending the U.S. air transportation system against chemical and biological threats*, Washington, DC, The National Academies Press.
- Olsen, S.J., Chang, H.L., Cheung, T.Y., Tang, A.F., Fisk, T.L., Ooi, S.P., Kuo, H.W., Jiang, D.D., Chen, K.T., Lando, J., Hsu, K.H., Chen, T.J. and Dowell, S.F. (2003) Transmission of the severe acute respiratory syndrome on aircraft, *N. Engl. J. Med.*, **349**, 2416-2422.
- Skaggs, T.H. and Kabala, Z.J. (1995) Recovering the history of a groundwater contaminant plume: Method of quasi-reversibility, *Water Resour. Res.*, **31**, 2669-2673.
- Tikhonov, A.N. and Arsenin, V.Y. (1977) *Solutions of ill-posed problems*, Washington, DC, Halsted Press.
- Wilson, J.L. and Liu, J. (1994) Backward tracking to find the source of pollution, *Water Manage. Risk Remed.*, **1**, 181-199.
- Zhang, T. and Chen, Q. (2007a) Novel air distribution systems for commercial aircraft cabins, *Build. Environ.*, **42**, 1675-1684.
- Zhang, T. and Chen, Q. (2007b) Identification of contaminant sources in enclosed environments by inverse CFD modeling, *Indoor Air*, In press.